

# Reconstructing Deepwater Channel-Lobe Depositional Environment in Highly Complex Multi-Gravity Flow to Traction Flow Deposits Using Borehole Image, Core and NMR Logs in Yinggehai Basin, South China\*

Shusheng Guo<sup>1</sup>, Bo Liu<sup>2</sup>, Jun Cai<sup>1</sup>, Hongjun Yang<sup>1</sup>, Yongde Gao<sup>1</sup>, Qingzhi Lu<sup>2</sup>, Vladimir Kuznetsov<sup>2</sup>, Huimin Cai<sup>2</sup>, Yuxi Wang<sup>2</sup>, Yanming Tong<sup>2</sup>, and Xianran Zhao<sup>2</sup>

Search and Discovery Article #41462 (2014)

Posted October 27, 2014

\*Adapted from extended abstract prepared in conjunction with oral presentation given at AAPG International Conference & Exhibition, Istanbul, Turkey, September 14-17, 2014, AAPG © 2014

<sup>1</sup>CNOOC Zhanjiang-Ltd., China

<sup>2</sup>Schlumberger China Petroleum Institute, China ([bliu7@slb.com](mailto:bliu7@slb.com))

## Abstract

In recent years, operators have drilled more than 20 appraisal wells to evaluate and characterize a gas reservoir in the Upper Miocene Formation in southern China's Yinggehai Basin. However, there is still no consistent understanding of the reservoir's depositional environment. This area is thought to have been developed by a vertically and laterally superposing multi-gravity flow deposit; thus, previous deposits exposed frequent denudation, forming a highly complex and heterogeneous reservoir. Both gravity flow and traction flow sedimentary features were found, and inadequate interpretation of the depositional environment failed to unravel the petrophysical property differences and reservoir thickness variation. Therefore, reconstructing the depositional environment is imperative.

We integrated borehole image, core, and nuclear magnetic resonance (NMR) log data to fully reconstruct the depositional environment in an adaptive approach. To efficiently achieve this, core and borehole images were calibrated to complement each other in analyzing lithology and sedimentary structure, then NMR and core data were calibrated to give an accurate petrophysical parameter. Results show that the channel-lobe depositional environments were involved in multi-gravity flow (debris flow and turbidity flow) and traction flow (internal wave and tide). Based on the newly reconstructed depositional environment, channel lobes were reclassified into three subcategories: internal wave and tide, gravity flow, and reworked internal wave and tide. In addition, sedimentary sequences were clearly defined from the bottom up: internal wave and tide (reworked) deposit (S1), debris flow deposit (S2), internal wave and tide (reworked) deposit (S3), and pelagic shale deposit (S4). The reconstructed channel-lobe depositional environment is a new breakthrough; it is essential for the generation and significant improvement of a new geological model. Future field development will be greatly improved because horizontal well trajectories can be placed in more favorable sedimentary sequences.

## Geological Background

The S area is located in the central uplift of the Yinggehai Basin offshore southern China. It is divided into SE and SY subareas, and the target formation is Upper Miocene. The lithology is mainly gray to light gray very fine- to fine-grained sandstone, with less medium-fine sandstone and shaly siltstone.

In the early exploration stage, the operator drilled exploration wells in the structural high, which is located in the SY area, but gas shows were very low. Then the operator drilled delineation wells in the structural low, which is in the SE area, and gas shows were very high. These results were the opposite of what was expected. How could they find higher gas shows in the lower structure?

Additionally, the sedimentary facies have inspired long-term debate. Some researchers interpreted the sedimentary facies as traction flow/delta front deposits because core photos show some traction flow features, such as flaser, wavy, and lenticular bedding. Other researchers interpreted it as gravity flow/submarine fan deposits with graded bedding, load structure, and floating mud-clasts. The sedimentary facies controlled a multiple gas reservoir system, which is featured by variable gas-water contact (GWC) and free-water level (FWL). [Figure 1](#) shows that wells in the SE area have a relatively deeper depth GWC and FWL, while wells in the SY area have a shallower depth.

### Identification of Gravity Flow and Traction Flow

Gravity flow is triggered by gravity, causing sediment flow only downslope. Traction flow is quite common in the subaerial environment, such as fluvial and alluvial deposits. Traction flow in the subaqueous environment (i.e. deepwater), however, are still under investigation in recent years. Traction flows have multiple directions, they may move downslope, upslope and along slope. As the origin of traction flow is from bottom current in deepwater, Shanmugam et al. (1993a, 2000a, and 2003) summarized the differentiation of bottom current and turbidity current in different aspects. Based on that, we extracted and refined from the following perspectives:

- Traction flows persist for long periods of time and can develop equilibrium conditions, whereas gravity flows are episodic, surge-type or mass movement events that fail to develop equilibrium conditions.
- Traction flows are free of sediment, and for this reason they are termed as ‘clear water currents’ (Bouma and Hollister, 1973, p. 82); whereas gravity flows cannot exist without entrained sediment.
- Traction flows show oscillating energy conditions, whereas gravity flows exhibit flow transformation energy conditions.
- Traction flows transport sand primarily by traction (i.e. bed load movement by sliding, rolling, and saltation; Allen, 1984), whereas gravity flows transport sediment by gravity and include a wide range of grain size sediments in different mechanism, i.e. turbidity currents transport fine-grained sand and mud in suspension, debris flows transport gravel-mud by plastic rheology and laminar state, which deposition occurs through freezing en masse.

Based on the core photo and borehole image, we summarized the traction flow and gravity flow sedimentary features separately. The traction flow features observed from core include flaser, wavy and lenticular bedding, double mud layer, bidirectional sand bedding, offshoot mud flaser and discontinuous mud flaser. Integrating with the local setting, it is found that the paleo-water depth, grain size and sediments color are very close to the conditions that internal wave and tide deposits can retain (LaFond, 1962; Munk, 1981; Gao et al., 1991; Yang et al., 2013). Internal wave and tide was firstly proposed by Gao and Eriksson (1991). Here we proposed a new concept of “internal wave and tides” in the S area to discern the root cause of petrophysical property variation ([Figure 2](#)).

In addition, gravity flow features from core observation are graded bedding, load deformed bedding, massive bedding, and scour surface, floating mud-clasts and amalgamated bedding (multi-graded bedding stacking) ([Figure 3](#)). Gravity flow deposits were periodically accompanied with internal wave and tides or reworked by internal wave and tides to a certain degree (Yang et al., 2013). As the paleo-water depth ranges from 100 m to 200 m, we considered sedimentary background is a submarine fan which is involved with both gravity flow and traction flow in the S area.

### **Channel-Lobe Characterization**

A submarine fan is composed of multiple sedimentary processes, and different flow transformations may occur among different processes. Conventionally, a submarine fan is divided into a channel, lobe, spray and levee, however, this facies classification does not adequately reveal the facies-related reservoir properties. To get a full understanding of the relation between facies and process, we divided submarine fan facies based on gravity flow and internal wave and tide flow. The later one is one type of bottom currents that developed in the research area. Thus, three main channel-lobe categories were characterized from lithology, dip features, sedimentary structure and top/bottom contact feature, gamma ray shape, reservoir thickness, seismic reflection, porosity and permeability. Lithology is based on core photos, mud logging and conventional logs. Dip features, sedimentary structures and top/bottom features are observed from both borehole image logs (FMI) and core photos. Gamma ray shape and reservoir thickness are from conventional logs, seismic reflection is from seismic profile. The reservoir porosity and permeability are derived from NMR logs after calibration with core data.

#### **(1) Gravity Flow Channel-Lobe**

Commonly, gravity flow includes sandy debris flow, muddy debris flow and turbidity flow (Shanmugam, 1996, 2000). He considered the high density turbidity current (Lowe, 1982) as sandy debris flow, which is a modified concept based on Shultz (1984).

- Main sandy debris flow channel: Lithology is fine to very fine sandstone; chaotic dips, mid to very high dip angle, or mid to high red pattern; box shaped gamma ray; 50-80 m thickness; medium to weak amplitude at top and bottom, internally weak amplitude, medium continuity and "V" or "U" incision seismic reflection; average porosity is 17.8%, range is 13%~26%, average permeability is 1.85 mD, range is 0.1~10 mD ([Figure 4](#)).

- Distributary sandy debris flow channel: Lithology is medium-fine sand, silty-fine and argillaceous sand; slightly changed dip, mid to high angle, red pattern; massive, deformed, floating mud clasts and reactivation surface, normal and reverse bedding; bell or funnel shaped gamma ray; 6-30 m thickness; medium to strong amplitude, medium to weak continuity and small scale “V” or “U” shape seismic reflection; average porosity is 18.4%, range is 10%~23%, average permeability is 13.43 mD and range is 0.1~100 mD ([Figure 5](#)).
- Sandy debris flow lobe: Lithology is silty-fine or fine sand; medium angle, stable green pattern or blue pattern; amalgamated and reverse graded bedding, sharp top and bottom contact; funnel and micro jagged shaped gamma ray; 1.5-16 m thickness; strong amplitude, discontinuous blocked seismic reflection; average porosity is 18.5 % and range is 7.5 %~22.5 %, average permeability is 6.02 mD and range is 0.5~40 mD ([Figure 6](#)).
- Muddy debris flow channel: Lithology is shale or silty shale; medium-low angle, not stable or slightly chaotic dip distribution; slump, massive structure, scour surface, load structure, and micro deformed bedding; micro jagged box shaped gamma ray, high value; 7-40 m thickness; medium-week amplitude, medium continuity, obvious “V” incision and internal chaotic seismic reflection; non-reservoir ([Figure 7](#)).
- Debris flow channel: Lithology is mud, sand and conglomerate mixed, variable grain size; medium-high angle deformed, chaotic distribution; slump, angular, striped or teared chaotic mud clasts distribution, strong scour surface and sharp top and bottom contact; irregular, high value gamma ray; 1.8-3.8 m thickness; average porosity is 12.6%, range is 9%-20%, average permeability is 1.7 mD, range is 0.01~31 mD ([Figure 8](#)).
- Turbidite channel: Lithology is fine sand and silty-fine sand; medium angle, red or green pattern; scour surface, normal graded bedding; bell shaped gamma ray; 1~2.5 m thickness; average porosity is 18.4%, range is 10.5~22.6%, and average permeability is 3.64 mD, range is 0.2~10 mD ([Figure 9](#)).

## (2) Internal Wave and Tide Channel-Lobe

- Internal wave and tide channel: Lithology is medium-fine and fine sand; not stable dip angle, local dips are nearly 180° opposite or pinniform distribution, most dips are medium-low angle, slightly changed; sedimentary structures contain bidirectional sand ripples, associated bedding (double/offshoot mud layer) and normal grading; mixed jagged bell or box shaped gamma ray, low value; 1-16 m thickness; medium-weak amplitude, poor continuity and parallel seismic reflection; average porosity is 17.3%, range is 10%~20%, and average permeability is 51.80 mD, range is 10~150 mD ([Figure 10](#)).
- Internal wave and tide lobe: Lithology is fine sand, argillaceous fine sand and medium to fine sand; medium-low angle dip, not stable, green pattern or blue pattern; mixed bedding (wavy and lenticular) and heterolithic bedding; slightly jagged funnel or bow shaped gamma

ray; 1-11 m thickness; strong amplitude, good continuity and parallel seismic reflection; average porosity is 16.9%, range is 9%~21.5%, and average permeability is 30.76 mD, range is 3~100 mD ([Figure 11](#)).

### **(3) Internal Wave and Tide Reworked Channel-Lobe**

- Internal wave and tide reworked channel: Lithology is fine sand and silty-fine sand; gravity channel-fill feature remained, medium-low angle and red pattern dip; associated bedding, few low-angle scour surfaces; bell or box shaped gamma ray; 1~11 m thickness; medium-strong amplitude, medium-continuity and wavy seismic reflection; average porosity is 14.7%, range is 8.8%~21.1%, and average permeability is 15.47 mD, range is 3~50 mD ([Figure 12](#)).
- Internal wave and tide reworked lobe: Lithology is fine sand and argillaceous fine sand; medium-low angle, not stable dips; heterolithic bedding, bioturbated shale layer, distributing like tail; non obvious gamma ray shape, 1.7~14 m thickness; strong amplitude, good continuity and parallel seismic reflection; average porosity is 16.2%, range is 9.2%~19.9%, and average permeability is 13.60 mD, range is 3~80 mD ([Figure 13](#)).

### **Petrophysical Properties Summary**

As analyzed above, we find that the porosity of each facies is within 12%-18%, however the permeability is highly variable. The facies internal wave and tide channel, internal wave and tide lobe have highest permeability; while the facies internal wave and tide reworked channel, and internal wave and tide reworked lobe have moderate permeability. Other gravity flow facies, sandy debris flow lobe, debris flow channel, turbidity channel, distributary sandy debris channel and main sandy debris channel, have lowest permeability ([Figure 14](#)).

### **Sedimentary Sequences**

Yang et al. (2013) summarized five sedimentary sequences from core observation in this area. They are: (a) internal wave and tide sequence, (b) gravity flow sequence, (c) rhythmical sequence of internal wave and tide and gravity flow, (d) periodic gravity flow and internal wave and tide sequence, and (e) gravity flow reworked by internal wave and tide sequence. These sequences clearly demonstrate how internal wave and tide and gravity flow coexist and associate with each other, as well as how they interact with the change of sea level. However, the sequences do not indicate vertical relationships which may be applied to find potential good reservoir in other areas.

Using core calibrated borehole image and conventional logs (gamma ray), we first vertically identified four sequences. From the bottom up: internal wave and tide (reworked) deposit (S1), debris flow deposit (S2), internal wave and tide (reworked) deposit (S3), and pelagic shale deposit (S4). S1 and S3 might be internal wave and tide deposit or internal wave and tide reworked deposits, However, S3 is easily retained by pelagic shale above, so it is thicker and more potential reservoir, both S1 and S3 are determined by the sea level change and sandy sediment supply ([Figure 15](#)).

Conventionally, internal wave and tide is developed in deep water environment (water depth more than 100-200 m), if the paleo-water depth is less than 200 m, when it becomes shallower with the sea level change falls, the internal wave and tide would decrease gradually. As mentioned above, the internal wave and tide is a type of traction flow, it will rework the previously deposited sediments by constantly or periodically winnowing. Hubert (1964) proposed importance of bottom currents in redistributing sediments in modern oceans. If the previous deposits are mainly shaly sandstone (sandy debris flow with certain shale content), the shaly content will be redistributed as shale layer, offshoot shale flaser, or discontinuous shale flaser, in this case the sand would become much cleaner, forming a better gas reservoir. Overall, sea level rise plus efficient sandy sediment supply would result in good sand reservoir, which is internal wave and tide channel-lobe or internal wave and tide reworked channel-lobe. In general, two alternative criteria are favorable for internal wave and tide (reworked) deposit:

- (1) Internal wave and tide develop where there has been previously deposited sandy gravity flow sediments, the previous sediments would be reworked to better reservoir.
- (2) Internal wave and tide develop in the place where there is no previous sandy gravity flow deposit, but there is sandy sediment supply from the upper shelf or slope, it would also form better reservoir.

### **Conclusions**

- Internal wave and tide was first recognized in the S area as traction flow, it is associated or coexisted with gravity flow. Internal wave and tide can rework the gravity flow deposits, which would result in better reservoir quality.
- The channel-lobe environment in submarine fan was reconstructed and redefined as three main categories: gravity flow channel-lobe; internal wave and tide channel-lobe; and internal wave and tide reworked channel-lobe. The best reservoir is internal wave and tide channel-lobe.
- Four sedimentary sequences (S1, S2, S3, and S4) were summarized from the bottom up, S3 sequence is the best reservoir interval in vertical section.
- This was the first time that facies analysis was linked to petrophysical properties; this helps in understanding the facies-controlled reservoir logging response and can give operators a specific interpretation model that has extensional application in adjacent and similar gas fields.

### **Acknowledgements**

Thanks to CNOOC-Zhanjiang Ltd. and Schlumberger China Petroleum Institute (SCPI) for allowing us to publish this paper. Thanks to their valuable suggestions, especially thanks to senior geologist Gong Hong Jie and Somenath Kar and senior geophysicist Xue Fang Jian.

## References Cited

- Allen, J.R.L., 1984, Sedimentary structures, their character and physical basis: Unabridged one-volume, Elsevier, Amsterdam, The Netherlands, I, p. 593, II, p. 663.
- Bouma, A.H., and C.D. Hollister, 1973, Deep ocean basin sedimentation, *in* G.V. Middleton, and A.H. Bouma, eds., Turbidites and Deep-Water Sedimentation, Anaheim: SEPM Pacific Section Short Course, California, p. 79-118.
- Dott, R.H., 1963, Dynamics of subaqueous gravity depositional processes: AAPG Bulletin, v. 47, p. 104-128.
- Gao, Z.Z., and K.A. Eriksson, 1991, Internal tide deposits in an Ordovician submarine channel: Previously unrecognized facies?: *Geology*, v. 19/7, p. 734-737.
- Hubert, J.F., 1964, Textural evidence for deposition of many western North Atlantic deep-sea sands by ocean-bottom currents rather than turbidity currents: *Journal of Geology*, v. 72, p. 757-785.
- LaFond, E.C., 1962, Internal waves: *The Sea*, v. 1, p. 731-751.
- Lowe, D.R., 1982, Sediment gravity flows, II: Depositional models with special reference to the deposits of high-density turbidity currents: *Journal of Sedimentary Petrology*, v. 52, p. 279-297.
- Middleton, G.V., and M.A. Hampton, 1973, Sediment gravity flows: Mechanics of flow and deposition, Turbidites and Deep-Water Sedimentation, Anaheim, California: SEPM.
- Munk, W., 1981, Internal waves and small scale processes, *Evolution of Physical Oceanography*. Cambridge: Massachusetts Institute of Technology, p. 246-291.
- Sanders, J.E., 1963, Concepts of fluid mechanics provided by primary sedimentary structures: *Journal of Sedimentary Petrology*, v. 33, p. 173-179.
- Shanmugam, G., 1996, High density turbidity currents: Are they sandy debris flows?: *Journal of Sedimentary Research*, v. 66, p. 2-10.
- Shanmugam, G., 2003, Deep-marine tidal bottom currents and their reworked sands in modern and ancient submarine canyons: *Marine and Petroleum Geology*, v. 20, p. 471-491.
- Shanmugam, G., 2006, Deep-water processes and facies models: Implications for Sandstone Petroleum Reservoirs: Elsevier, Amsterdam, The Netherlands,

Shultz, A.W., 1984, Subaerial debris flow deposition in the upper Paleozoic Cutler Formation, western Colorado: *Journal of Sedimentary Research*, v. 54, p. 759-772.

Yang, H.J., S.S. Guo, and B. Liu, 2013, Gravity flow and internal wave and internal tide deposits in Upper Miocene of SE Area, Yinggehai Basin: *Petroleum Geology and Experiment*, v. 35/6, p. 626-633.



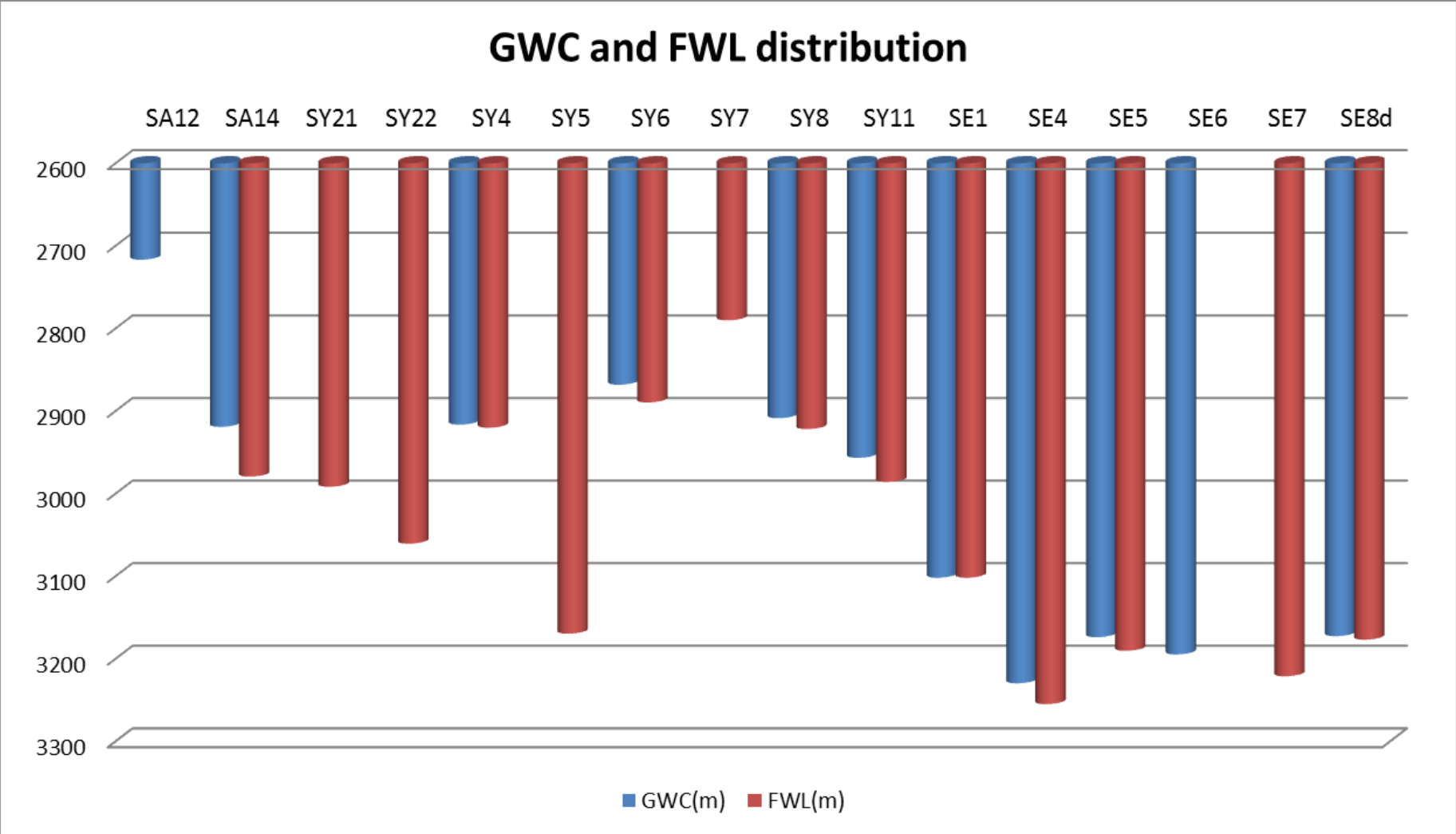


Figure 1. Gas-water contact (GWC) and free-water level (FWL) distribution in S area indicate a complex multiple gas reservoir system.

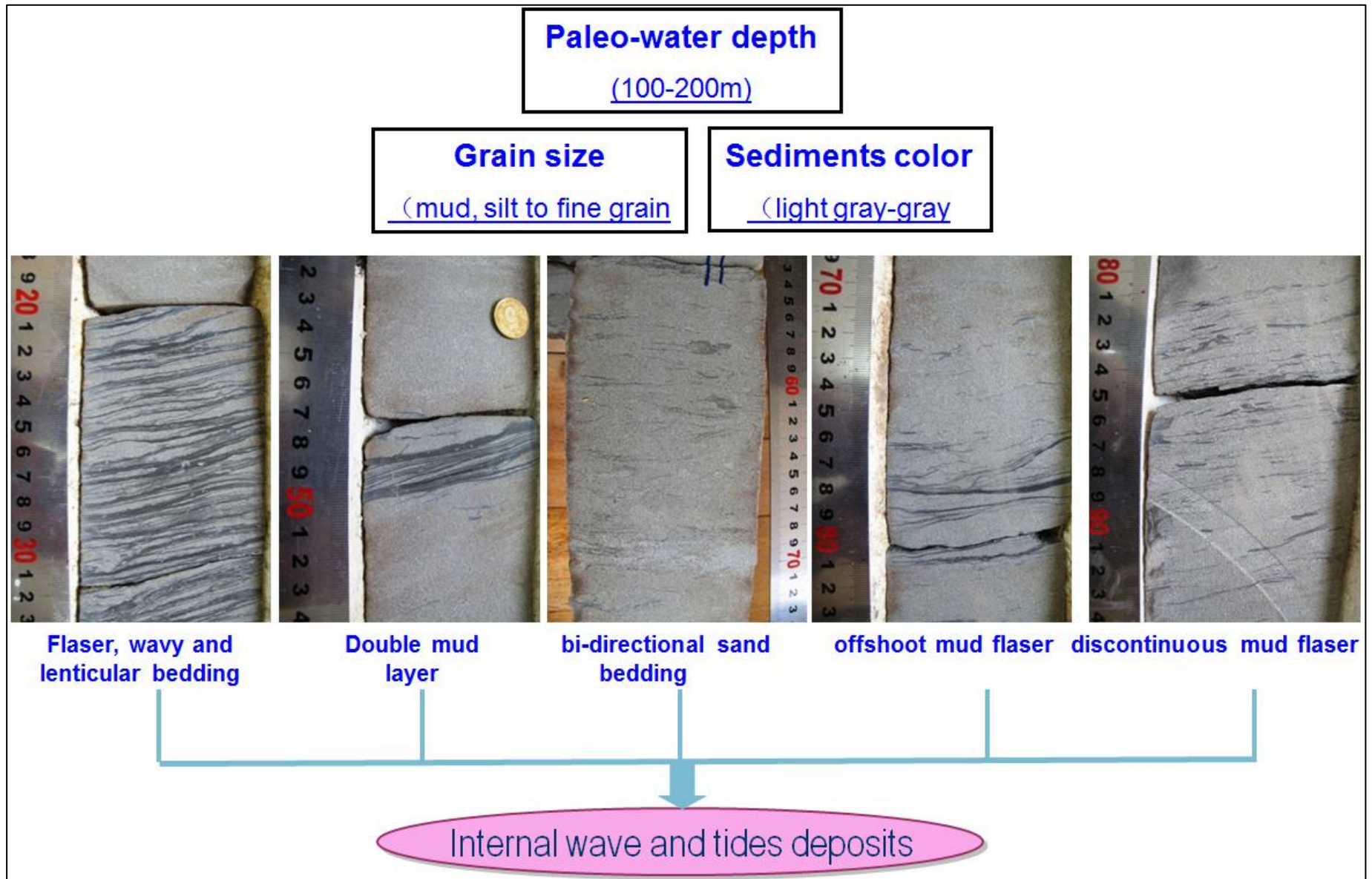


Figure 2. Novel proposed identification evidence of internal wave and tides deposits.

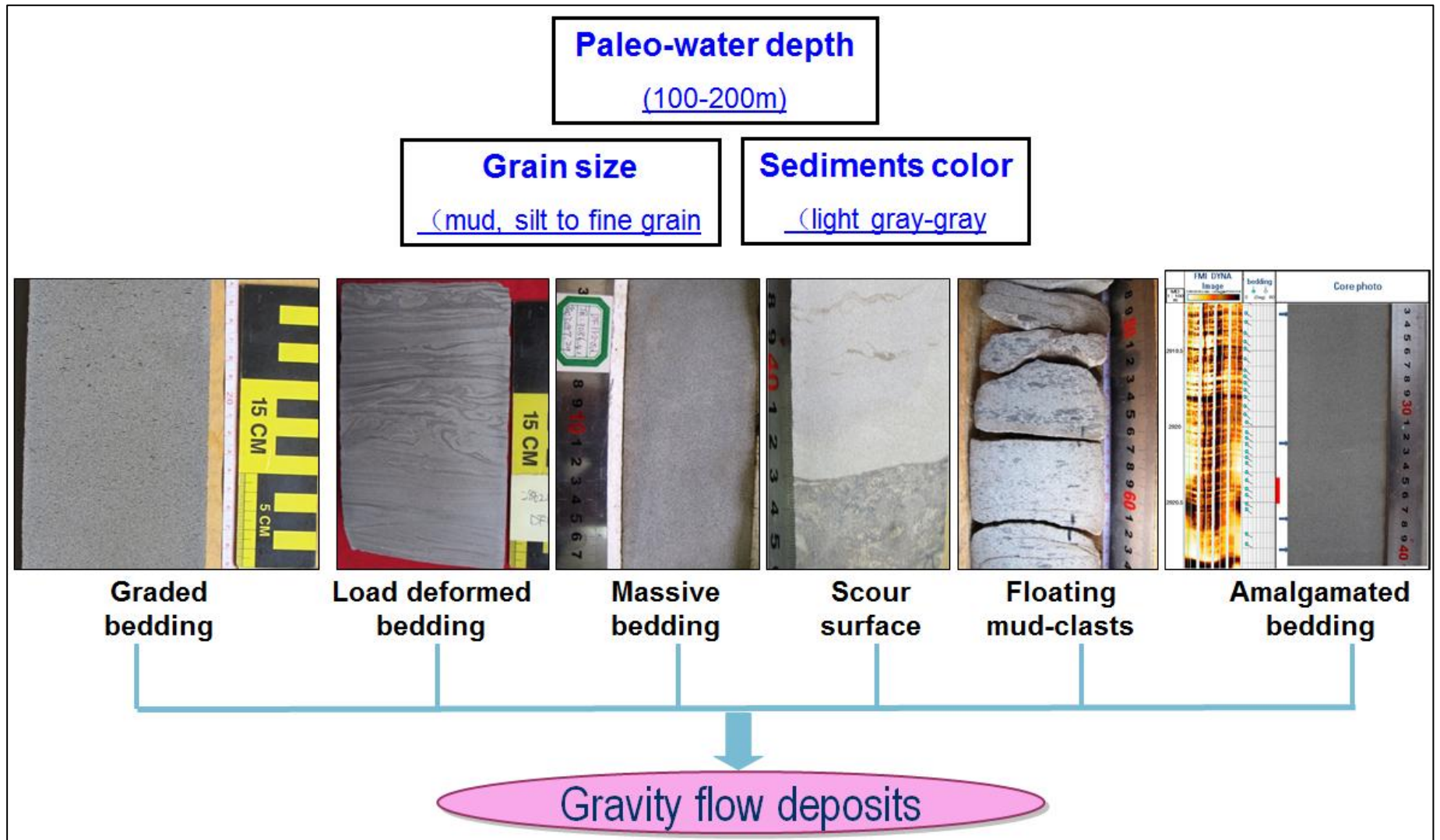


Figure 3. Novel proposed identification evidence of gravity flow deposits.

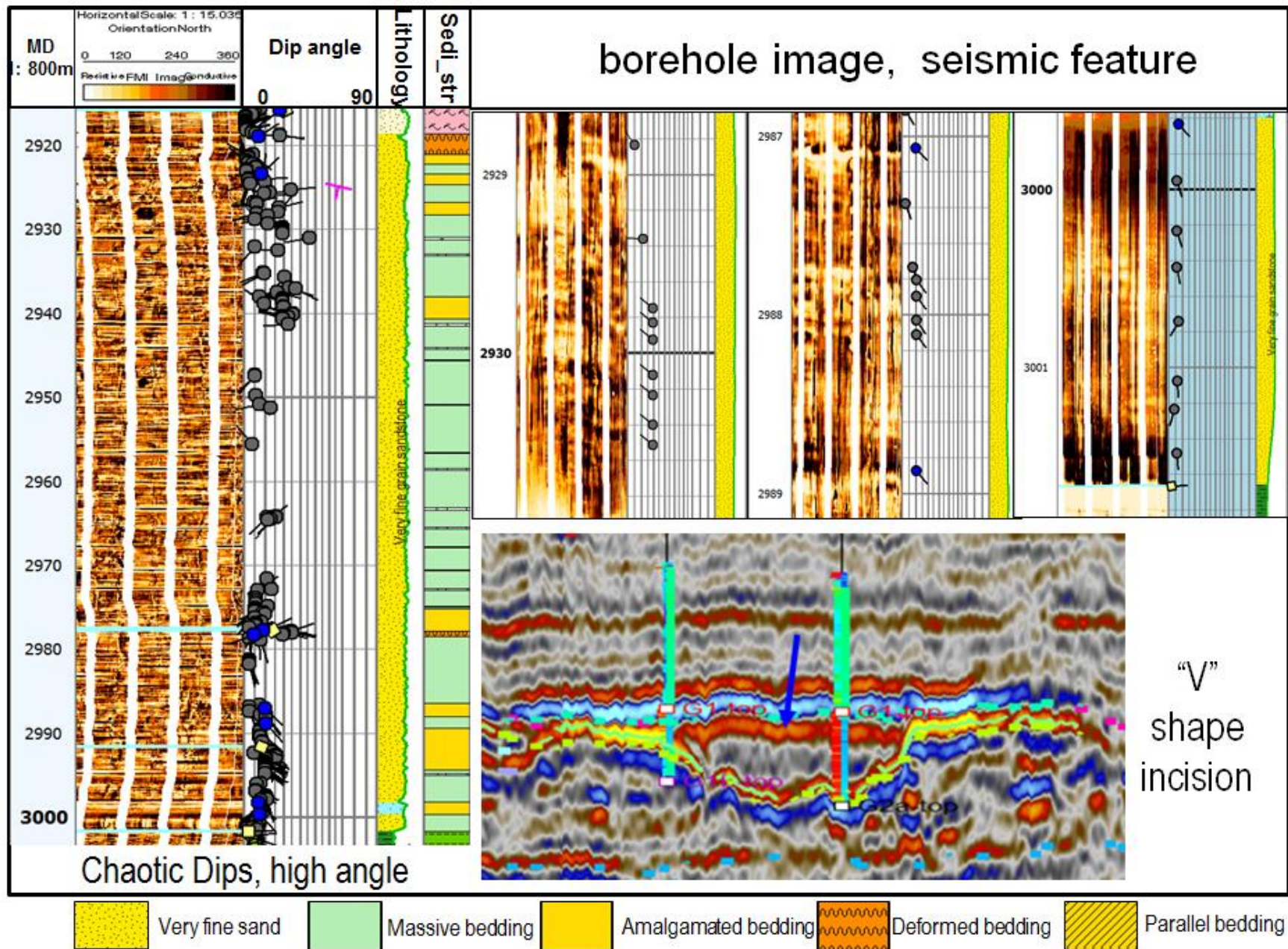


Figure 4. Main sandy debris flow channel characterization.

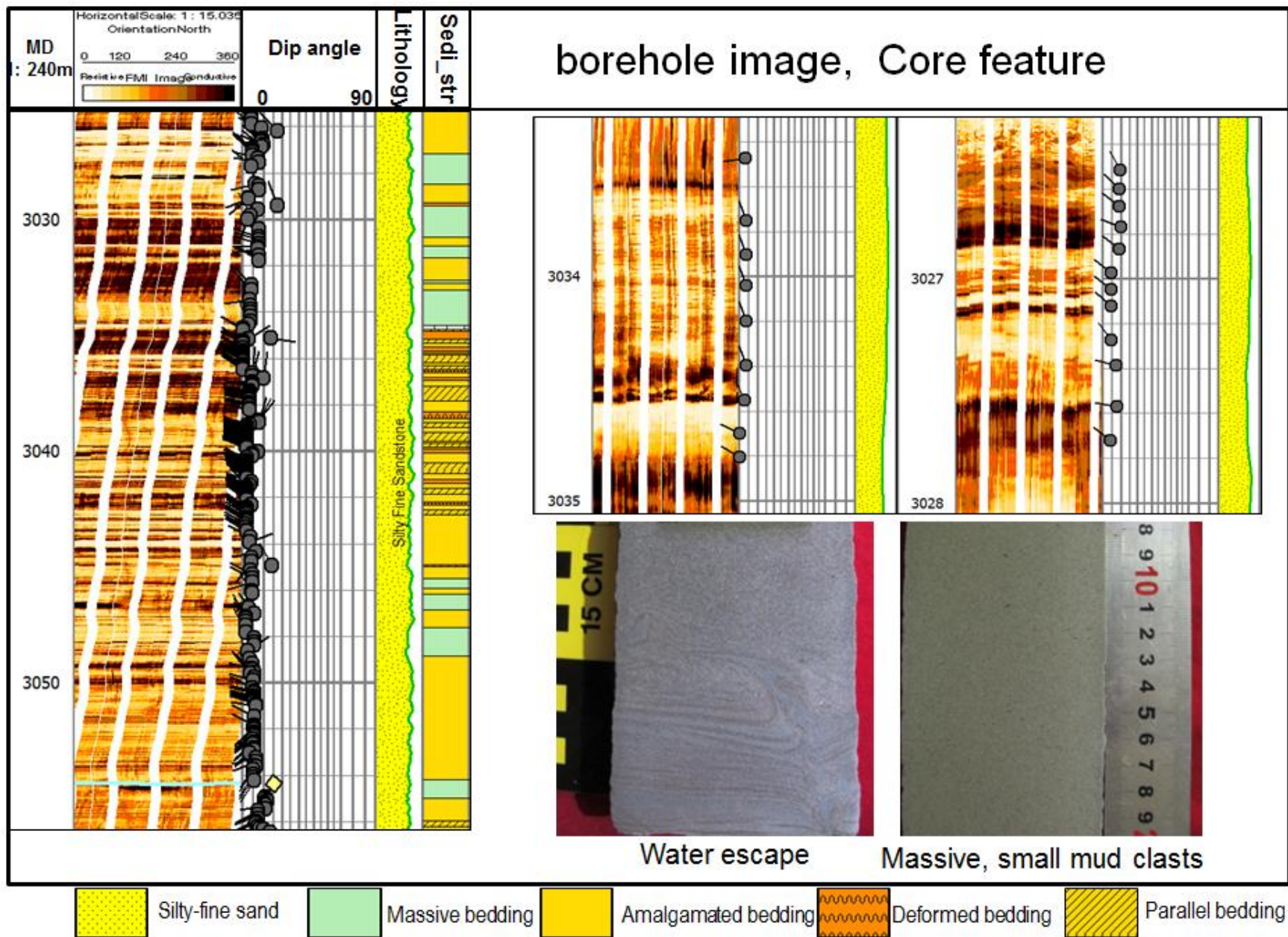


Figure 5. Distributary sandy debris flow channel characterization.

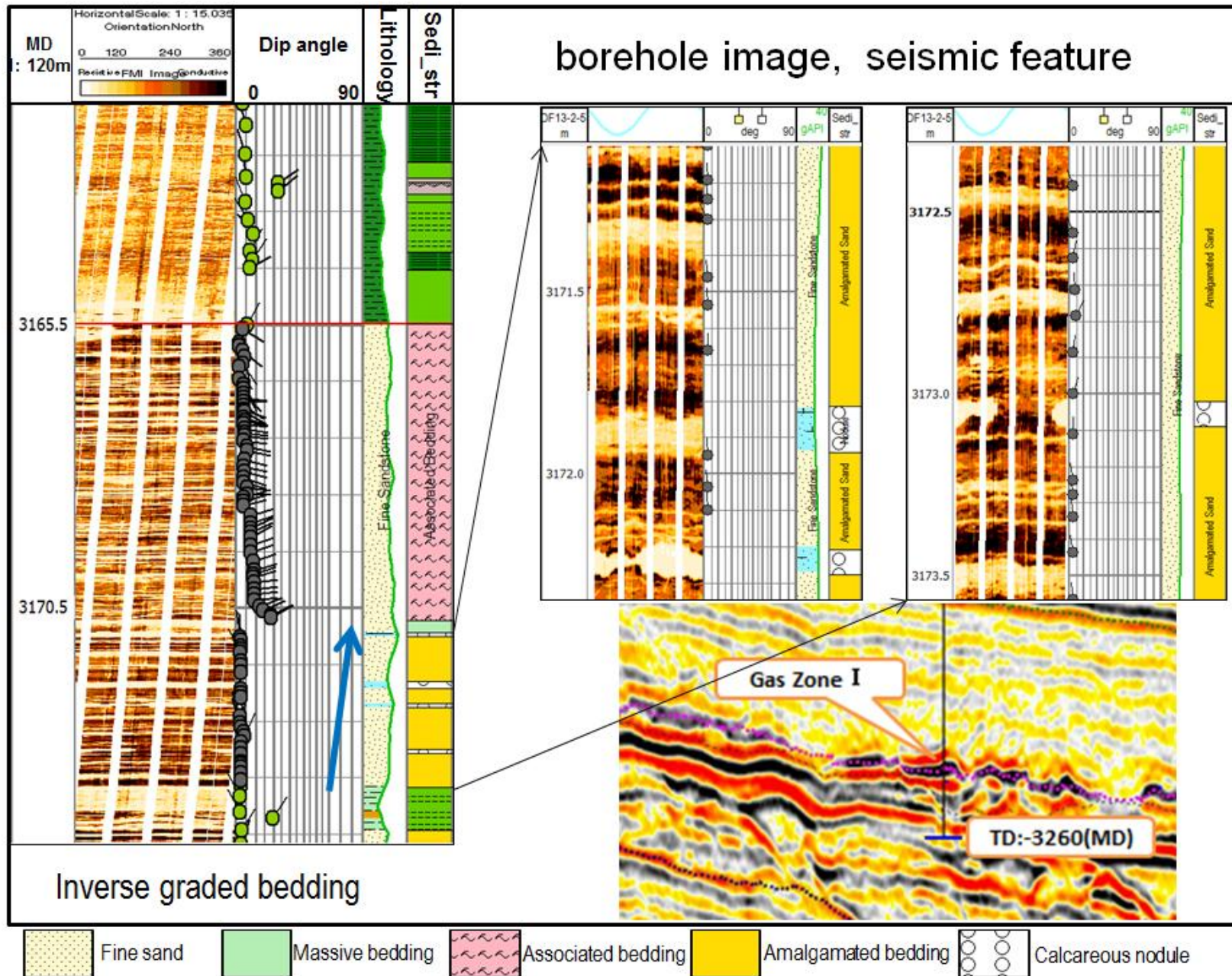


Figure 6. Sandy debris flow lobe characterization.

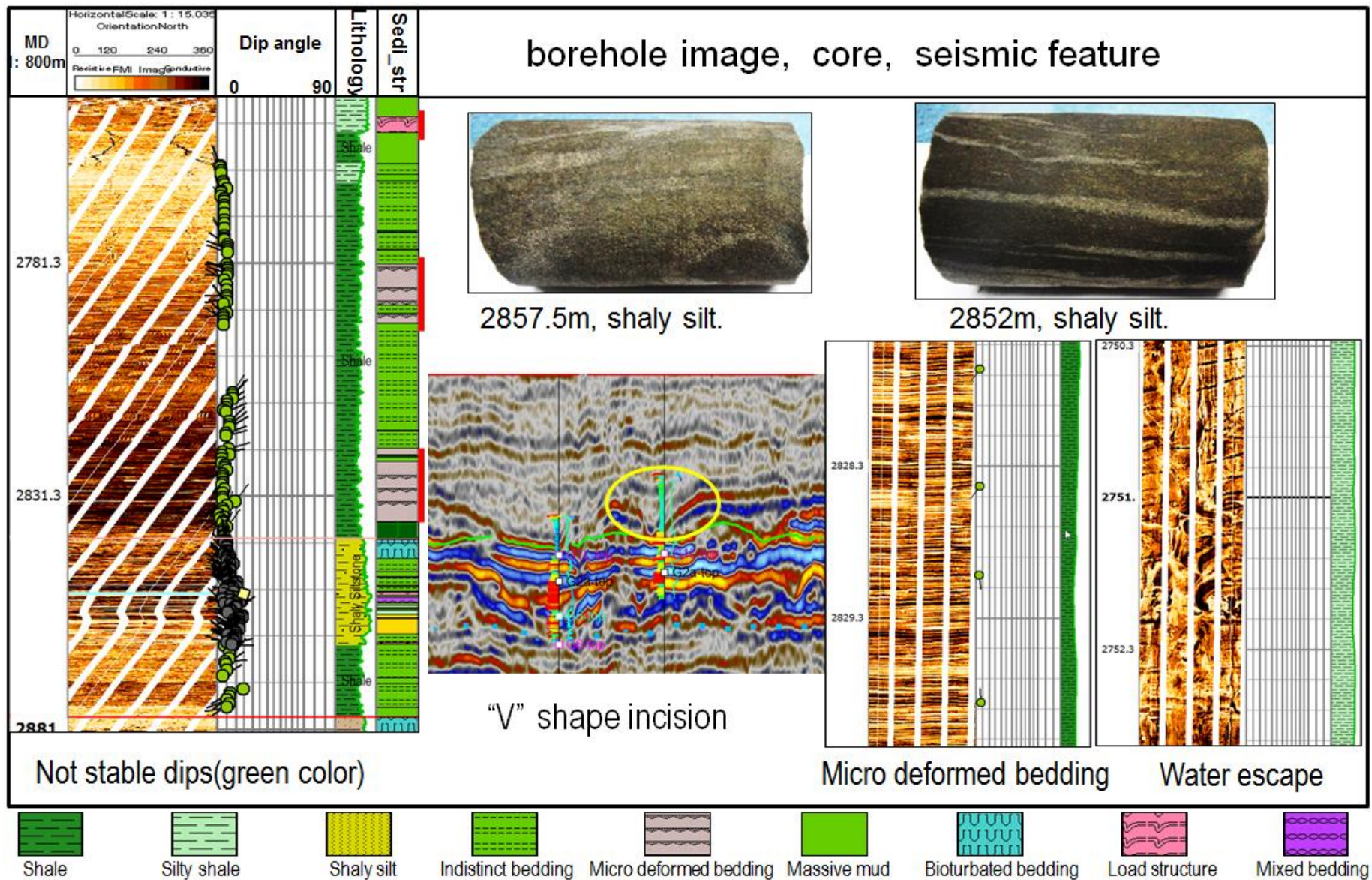


Figure 7. Muddy debris flow channel characterization.

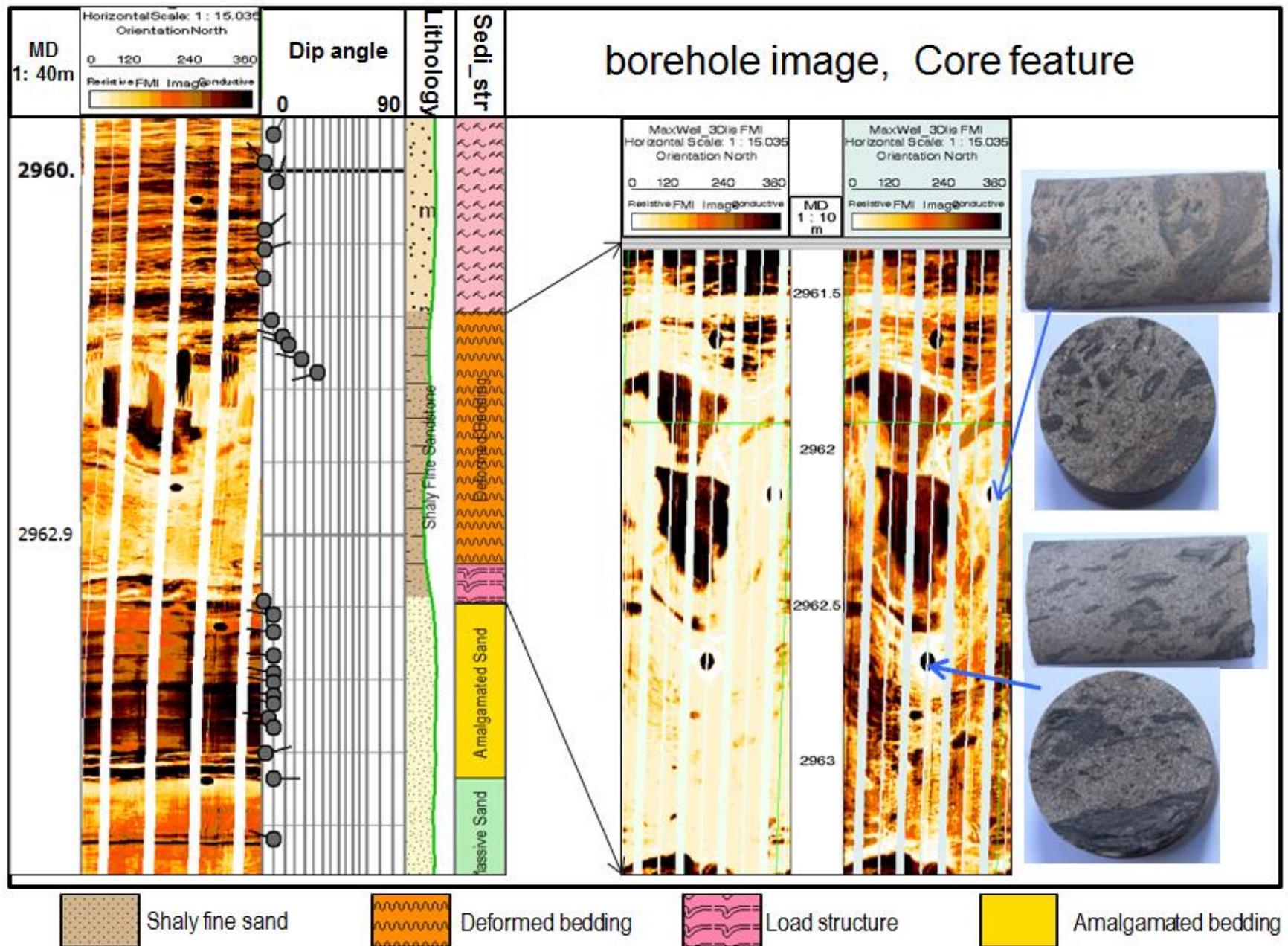


Figure 8. Debris flow channel characterization.



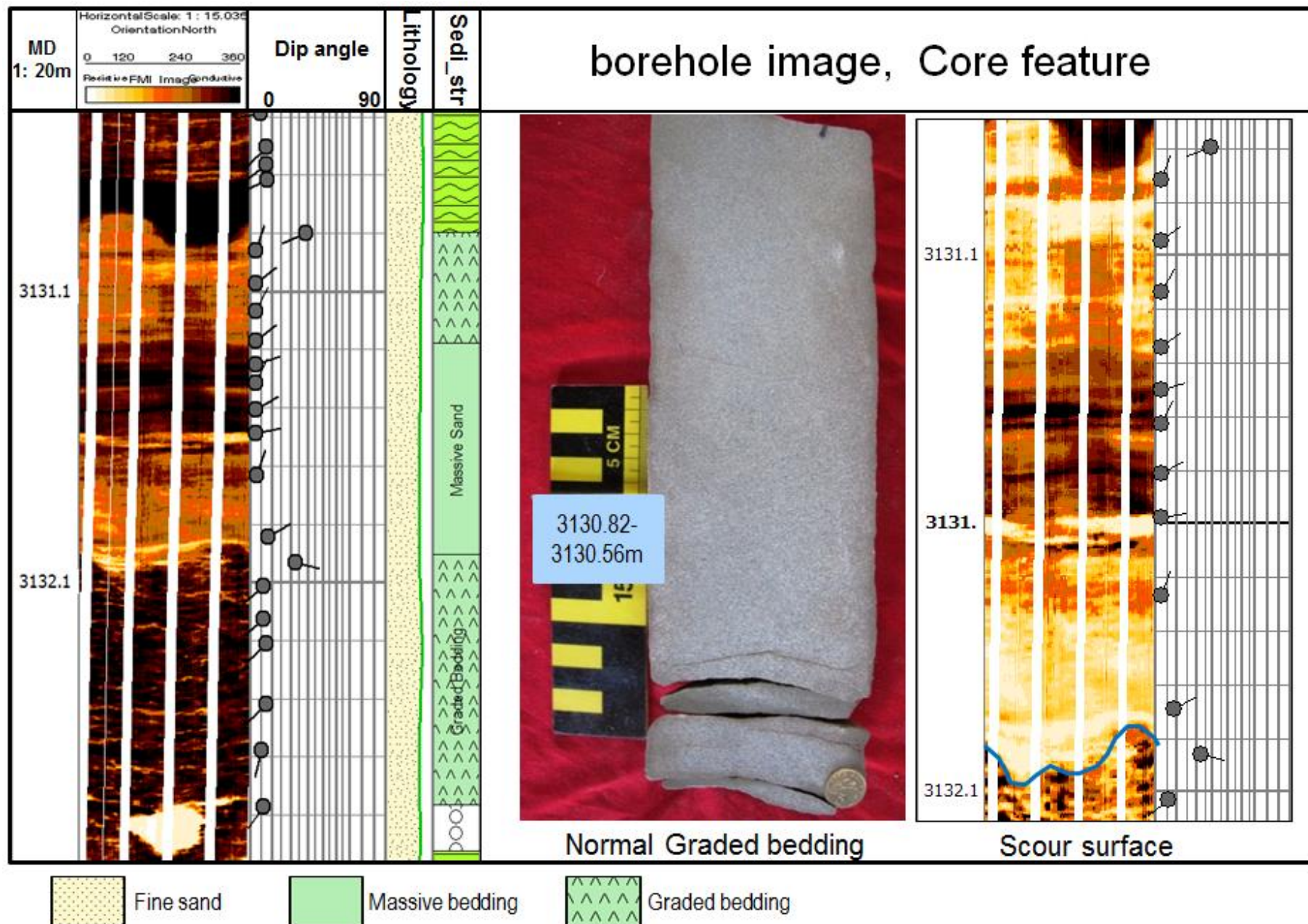


Figure 9. Turbidite channel characterization.

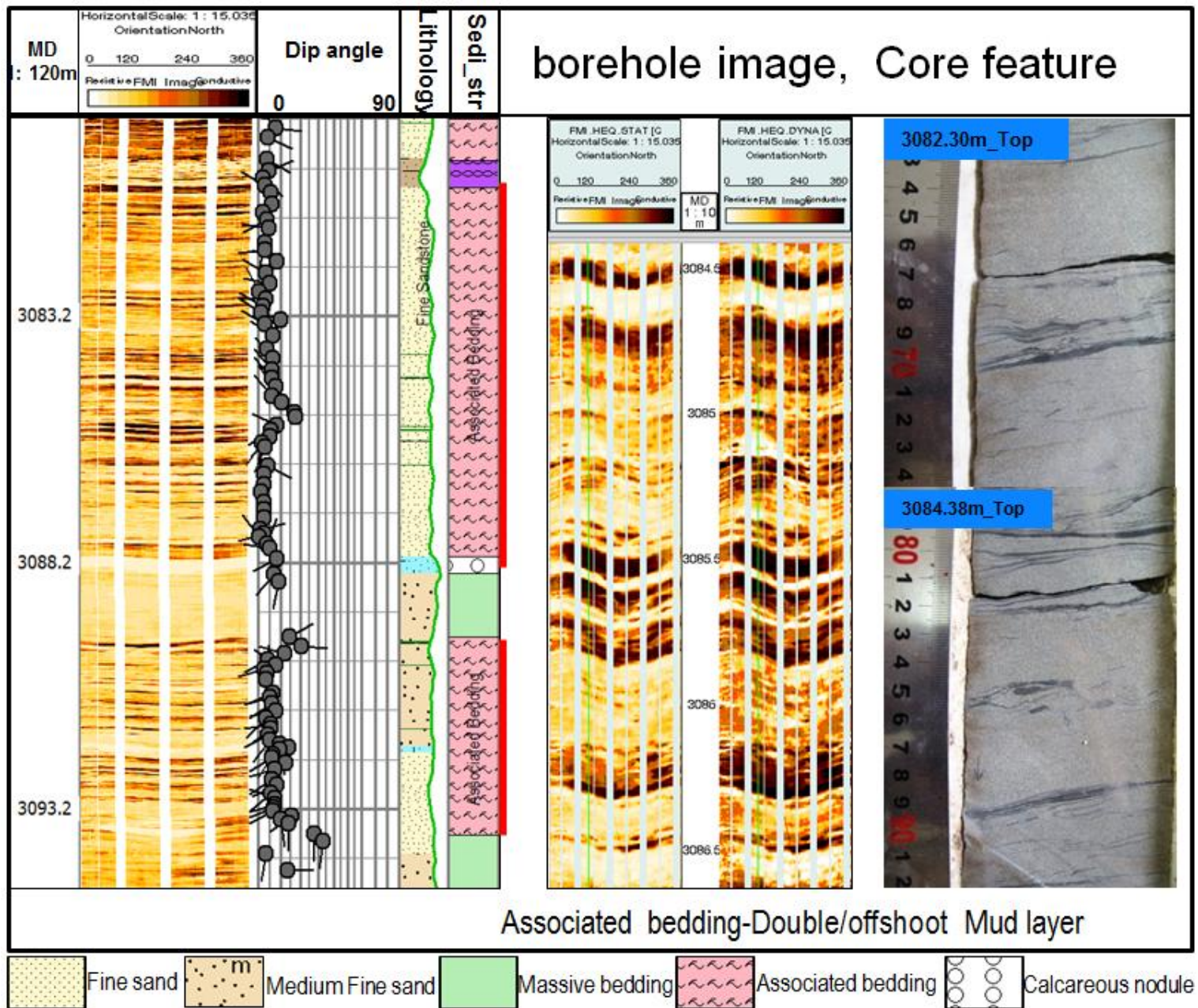


Figure 10. Internal wave and tide channel characterization.

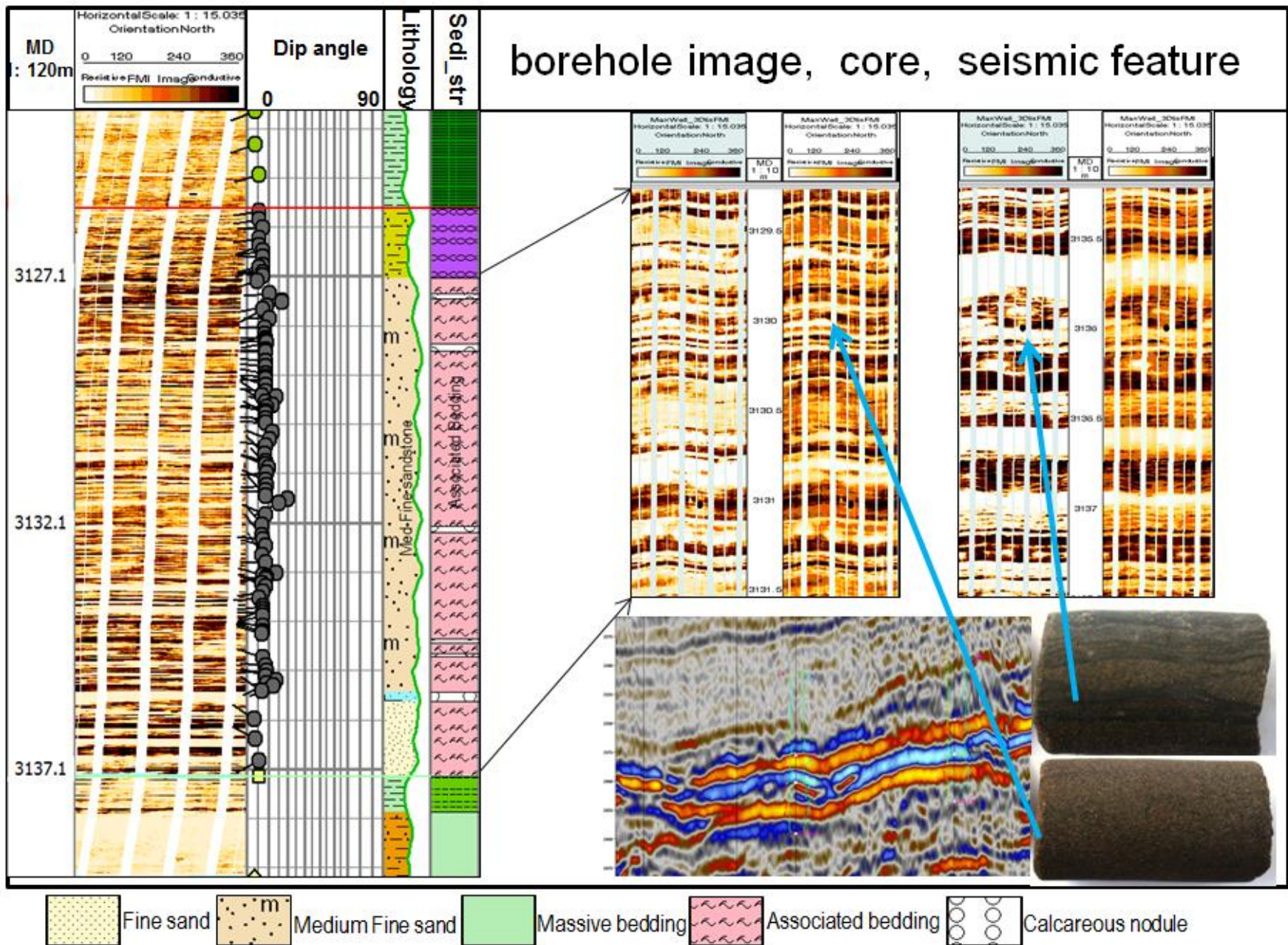


Figure 11. Internal wave and tide lobe characterization.

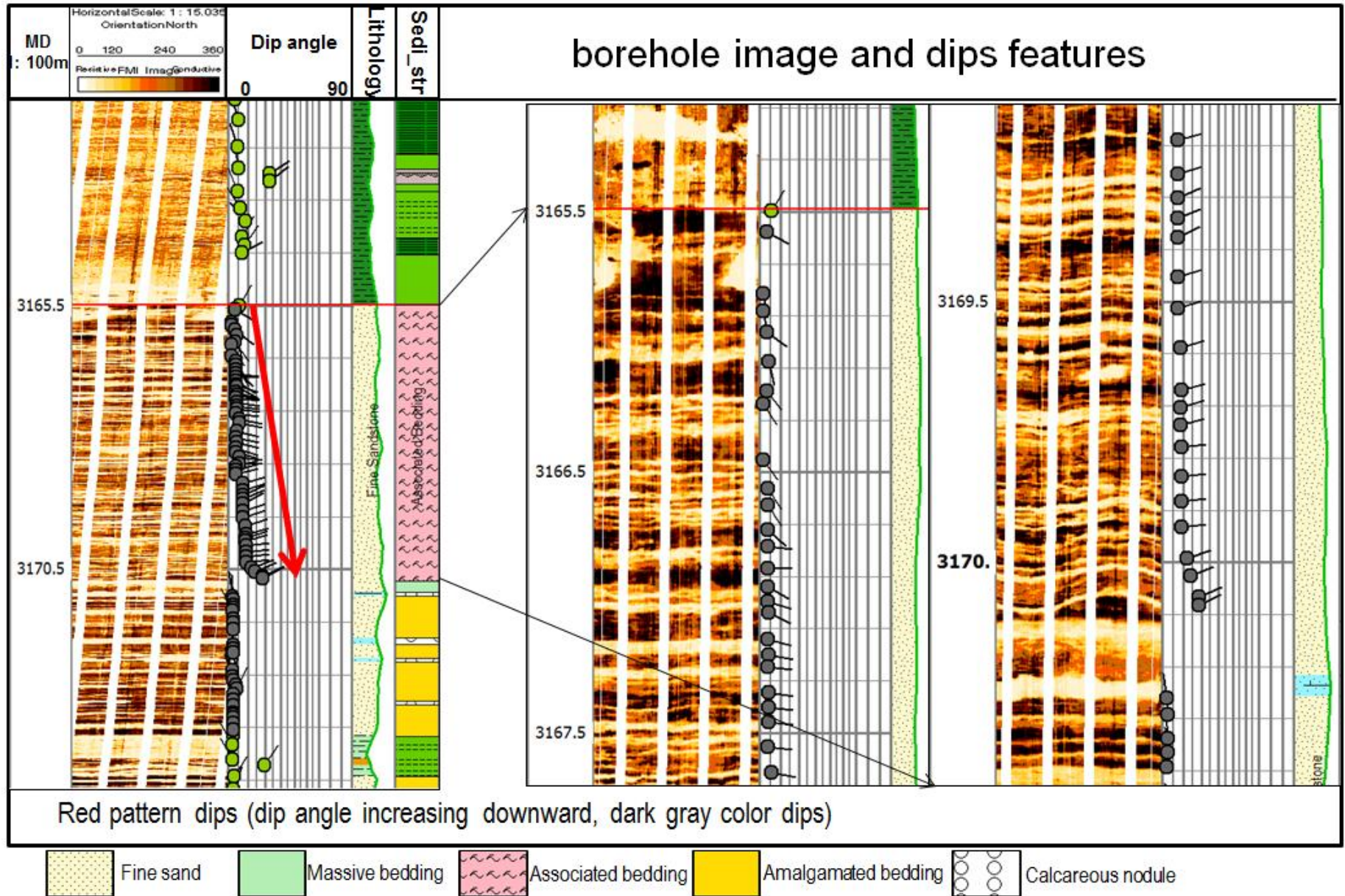


Figure 12. Internal wave and tide reworked channel characterization.

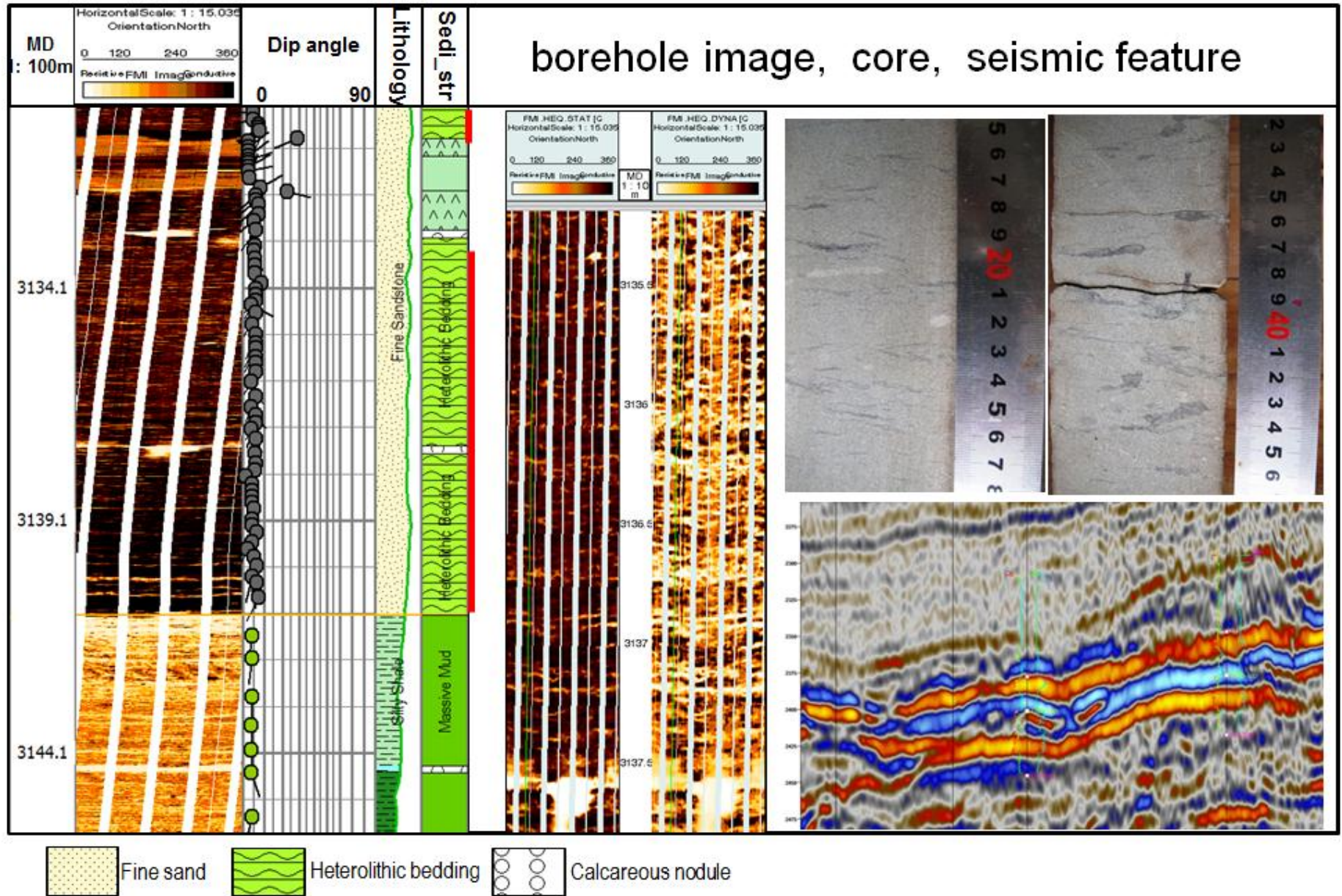


Figure 13. Internal wave and tide reworked lobe characterization.

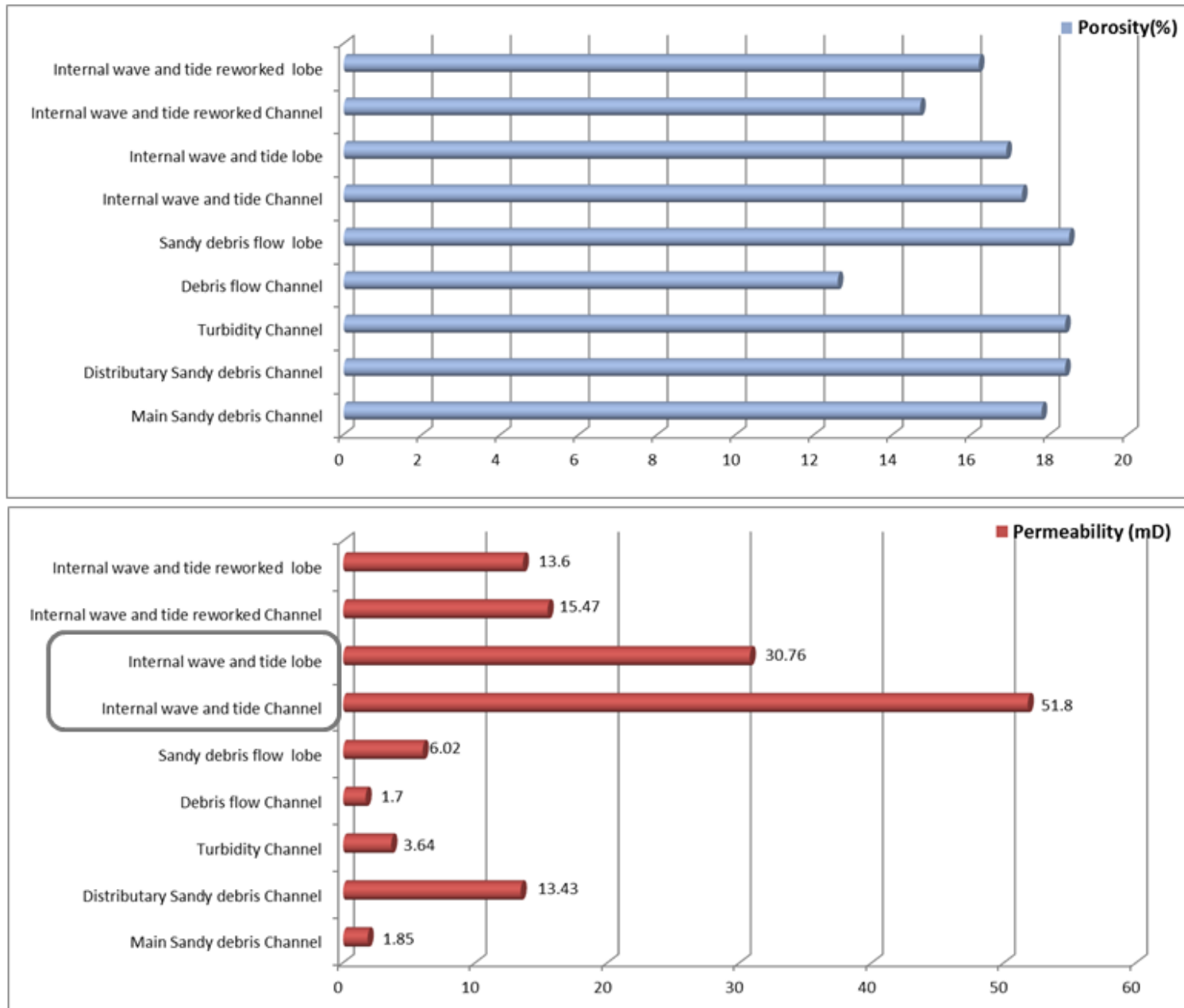
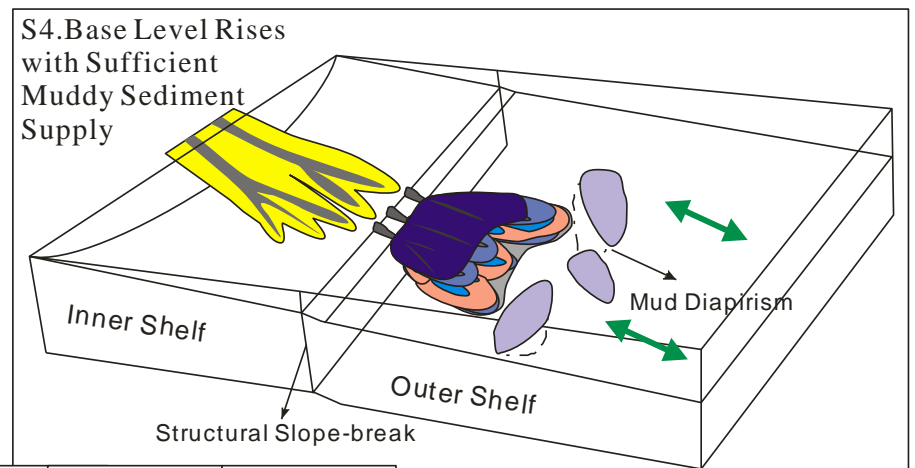
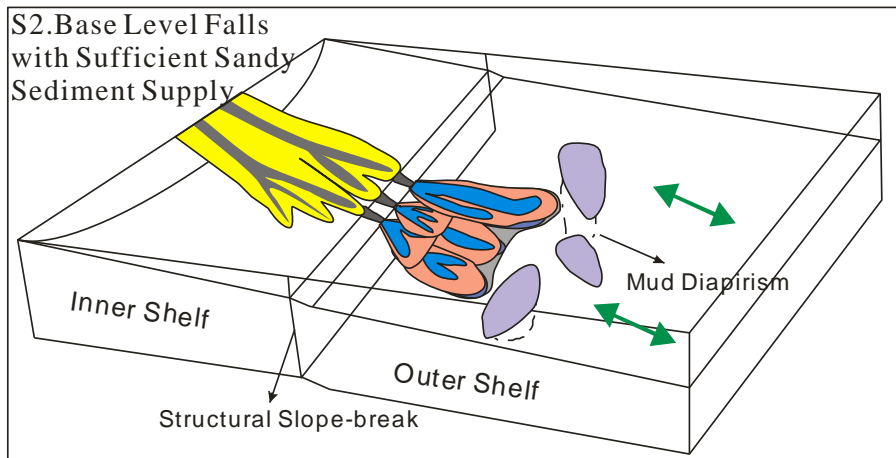
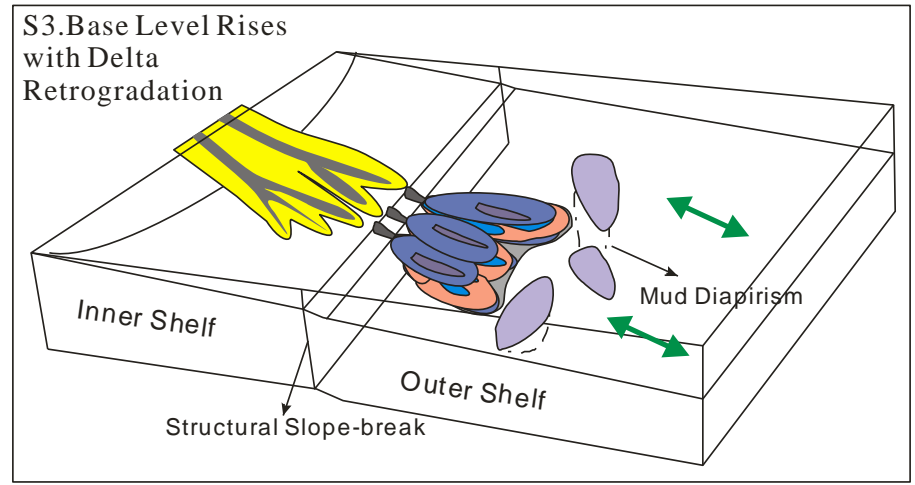
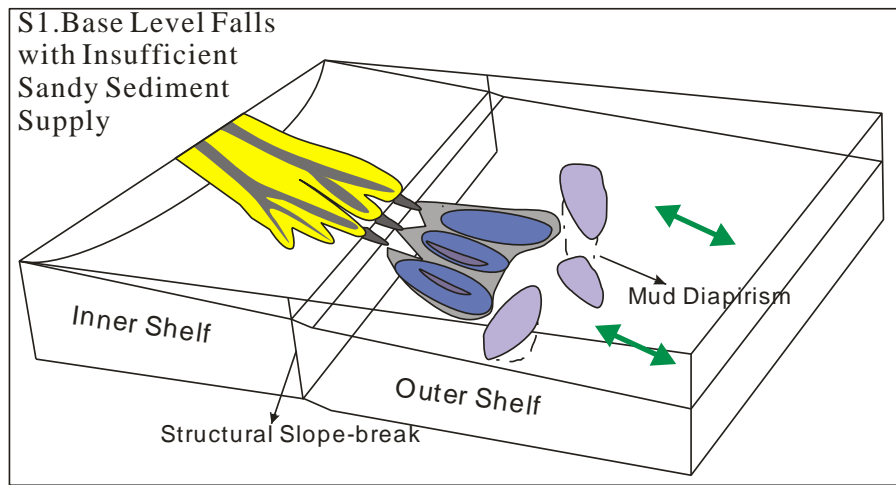


Figure 14. Summarized petrophysical property of different facies in the S area.



**Legend**

Upperfan Erosional Channel	Distributary Channel & Lobe	IWIT Reworked Distributary Channel & Lobe	Neritic Sea Shoal-bar	Mud Flow Gully	Neritic Sea Mud Deposits	Internal Wave-Internal Tide Flow

Figure 17. Summarized sedimentary sequences in the S area.